Published in final edited form as:
J Math Imaging Vis. 2006 January 31; 24(2): 209–228. doi:10.1007/s10851-005-3624-0.

Geodesic Shooting for Computational Anatomy

MICHAEL I. MILLER,
Center of Imaging Science & Department of Biomedical Engineering, The John Hopkins University, 301 Clark Hall, Baltimore, MD 21218, USA

ALAIN TROUVÉ, and
CMLA, ENS de Cachan, 61 Avenue du Président Wilson, 94235 Cachan CEDEX, France

LAURENT YOUNES
Center for Imaging Science & Department of Applied Math and Statistics, The Johns Hopkin, 3245 Clark Hall, Baltimore, MD 21218, USA

MICHAEL I. MILLER: mim@cis.jhu.edu; ALAIN TROUVÉ: trouve@cmla.ens-cachan.fr; LAURENT YOUNES: laurent.younes@jhu.edu

Abstract

Studying large deformations with a Riemannian approach has been an efficient point of view to generate metrics between deformable objects, and to provide accurate, non ambiguous and smooth matchings between images. In this paper, we study the geodesics of such large deformation diffeomorphisms, and more precisely, introduce a fundamental property that they satisfy, namely the conservation of momentum. This property allows us to generate and store complex deformations with the help of one initial "momentum" which serves as the initial state of a differential equation in the group of diffeomorphisms. Moreover, it is shown that this momentum can be also used for describing a deformation of given visual structures, like points, contours or images, and that, it has the same dimension as the described object, as a consequence of the normal momentum constraint we introduce.

1. Introduction

Over the past several years we have been studying natural shapes using homogeneous orbits of imagery constructed via the action of transformation groups on exemplars or templates. The mathematical structure of group action as a model in image analysis has been pioneered by Grenander [13], the idea being to introduce the group actions in the very nature of the objects themselves, through the notion of *deformable templates*. Roughly speaking, a deformable template simply is an "object or exemplar" I_{temp} on which a group G acts and generates, through the orbit $\mathcal{I} = G \cdot I_{\text{temp}}$, a whole family of new objects. The interest of this approach is to concentrate the modeling effort on the group G, and not on the family of objects $\mathcal{I}$.

Since the earliest introduction by Silicon Graphics Incorporated of special purpose graphics hardware for object rendering, group action as a model in image analysis has been the subject of a wide range of research in computer vision. Naturally, the analytical and computational properties of the low-dimensional matrix Lie groups form the core dogma of modern Computer graphics. In sharp contrast, however, for the study of imagery generated from natural or biological shapes, the finite dimensional matrix groups are replaced by their infinite dimensional analogue, the more general diffeomorphisms [7,11,16,22,23,36].

The anatomical orbit or deformable template is made into a metric space with a metric distance between elements by constructing curves through the space of diffeomorphisms connecting them; the length of the curve becomes the basis for the construction, the metric distance corresponding to the geodesic shortest length curves. This gives rise to a natural variational problem describing the geodesic flows between elements in the orbit, with the solution of the associated Euler-Lagrange equations giving the optimal flow of diffeomorphisms and thus the metric between the shapes. The obtained setting shares several similarities with the mechanics of perfect fluids, for which the Euler-Lagrange equation has been derived by Arnold (Eq. (1) of [2]) for the group of divergence-free volume-preserving diffeomorphisms. As well these results become another example of the general Euler-Poincaré principle of [19] applied to an infinite dimensional setting.

Interestingly, as emphasized by Arnold [1] in his study, one of the most beautiful aspects of studying diffeomorphisms with a Lie group point of view is that many fundamental aspects which can be proved in the finite dimensional case can be formally extended to retrieve well-known equations of mechanics. One of the purposes of this paper is to develop infinite dimensional analogues, for the study of high dimensional shapes via diffeomorphisms, of several of the well known properties of Lie groups in rigid body mechanics. In particular we shall focus on the interpretation of the Euler equation as an expression of the evolution of the generalized momentum of diffeomorphoc flow of least energy in both Eulerian and Lagrangian coordinates.

Such a point of view will link our geodesic formulation to a *conservation of momentum law* in Lagrangian coordinates providing a powerful method for studying and modeling diffeomorphic evolution of shape. It will imply that the momentum of the diffeomorphic flow at any place along the geodesic can be generated from the momentum at the origin, thus providing the vehicle for *geodesic generation via shooting*.

This same conservation of momentum of the diffeomorphic flow, allows us to derive equations for the geodesic evolution of the elements in the orbit $I_t = I \circ \varphi_t^{-1}$, $t \in [0, 1]$, $I \in \mathcal{I}$. This unifies various geodesic evolutions associated with orbits of sparse finite dimensional landmarked shapes as well as the evolutions of dense images. Of special interest is the fact that for the special case of image matching, geodesic evolution of elements in the orbit links us to the notion of normal motion familiar to the rapidly growing community working in *level set methods*. Interestingly, as we show, the momentum of the diffeomorphic flow is normal to the level sets associated with geodesic motion. By solving the partial differential equations which are associated with the conservation of momentum, we will be able to control by specifying the initial conditions (within a specific class of momentum which depends on the considered imaging problem) a wide range of arbitrarily large deformations; this provides new possibilities for learning shape models of deformable templates, or for designing new numerical matching procedures.

This second point of view in terms of the conservation of momentum law also sheds new light on a large number of high dimensional evolution based Active Model Methods in Computer Vision, including active snakes and contours [6,12,18,20,29,31,37,40,41,43], active surfaces and deformable models [8,9,21,24,25,28,30,33,39,40,42]. In such approaches vector fields are defined which give the boundary manifold of the shape some velocity of motion, usually following the gradient of an energy to form an attractive force to pull the boundary. The power of such methods is that they parameterize motion only associated with a submanifold of the imagery, not the entire extrinsic background space. For example, to deform a planar simply connected shape via an active contour method, the dimension of the motion is determined by the dimension of the boundary of the region, which is substantially less than the dimension of the plane. Historically such approaches have not been studied

globally as diffeomorphic action. In fact it is well known that such methods cannot prevent self intersection nor ensure topological consistency, for which the addition of other constraints become necessary [14,15]. From the conservation law in Lagrangian coordinates describing geodesic motion in the metric space of diffeomorphic action, we introduce the *normal momentum motion* which constrains the momentum to the bounding manifold, and extends the velocity of motion of the shape to the entire background space, thereby giving the global property that the resulting integrated vector field generates a diffeomorphism on the entire extrinsic space. This in turn carries the smooth submanifold diffeomorphically. As the analysis shows, this global property seems to be required to generate geodesic motions.

2. The Basic Set Up

2.1. Right Invariant Metric on Group of Diffeomorphisms

The basic component of our models is the group of one-to-one, smooth, transformations (diffeomorphisms) of a bounded subset $\Omega \subset \mathbb{R}^d$. In this paper, we consider diffeomorphisms emerging as flows of non-autonomous differential equations. A time dependent vector field on Ω is a function:

$$v:[0,1]\times\Omega\to\mathbb{R}^d$$
$$(t,x)\mapsto v(t,x)$$

($v(t, x)$ will also be denoted $v_t(x)$). The associated ordinary differential equation is

$$\frac{dy}{dt}=v_t(y).$$

The flow of this ODE is a function φ^v which depends on time and space, such that

$$\frac{\partial\varphi^v}{\partial t}(t,x)=v_t\left(\varphi_t^v(x)\right)$$

and $\varphi(0, x) = x$ for all $x \in \Omega$. We will also use the notation $\varphi_t^v(x)$ for $\varphi(t, x)$ and

$$\varphi_s^{v-1}=\varphi_t^v\circ\varphi_s^{v-1}. \tag{1}$$

It is well-known that, under some smoothness conditions on v, such φ_t^v is at all times a diffeomorphism of Ω.

The groups that we consider are precisely composed with such flows φ_1^v for v belonging to a specified functional class. More precisely, we assume that a Hilbert space $\mathcal{g}$ is given, the element of which being smooth enough vector fields on Ω, and denote the norm and inner product on this space by $\|\ \|_{\mathcal{g}}$, $\langle,\rangle_{\mathcal{g}}$. We now define (following [35]) the group G as the set of functions φ_1^v for time-dependent vector fields v satisfying

$$\int_0^1 \|v_t\|_{\mathfrak{g}} dt < \infty,$$

i.e. for v belonging to $L^1([0, 1], \mathfrak{g})$. We will always assume that $\mathfrak{g}$ can be embedded in the space of $(C_0^1(\Omega, \mathbb{R}^d), \| \|_{1,\infty})$, containing vector fields on Ω, which vanish on $\partial\Omega$, where

$$\|w\|_{1,\infty} = \|w\|_\infty + \|dw\|_\infty.$$

From this definition, it appears that the main ingredient in the construction of G is the Hilbert space $\mathfrak{g}$.

Fixing $v \in \mathfrak{g}$, one can define the linear form $w \mapsto \langle v, w \rangle_g$, which will be denoted Lv. We therefore have the identity

$$(Lv, w) \doteq \langle v, w \rangle_{\mathfrak{g}}$$

(we use the standard notation (M, w) for the linear form M applied to w). By definition, Lv belongs to the dual, $\mathfrak{g}^*$ of $\mathfrak{g}$, and L can be seen as an operator $L: \mathfrak{g} \to \mathfrak{g}^*$ (this is the canonical duality operator of $\mathfrak{g}$ on its dual). As we shall see, this operator turns out to be a key feature in our analysis. For the moment, we point out the fact that Lv is a linear form on $\mathfrak{g}$ which is a space of smooth vector fields. Therefore, Lv itself can be a singular object (a generalized function, or a distribution). Here are a few examples of distributions M which qualify as elements of $\mathfrak{g}^*$, under our running assumption that $\mathfrak{g}$ is embedded in the space of C^1 functions:

i. L^1 vector fields of Ω: if $\psi: \Omega \mapsto \mathbb{R}^d$ is integrable, define

$$(M, v) = \int_\Omega \langle \psi(x), v(x) \rangle_{\mathbb{R}^d} dx$$

ii. Let now μ be any measure on Ω, and ψ be μ integrable. Define

$$(M, v) = \int_\Omega \langle \psi(x), v(x) \rangle_{\mathbb{R}^d} d\mu(x)$$

iii. Dirac measures: as a particular case of the previous, define, for $x \in \Omega$ and $a \in \mathbb{R}^d$,

$$(M, v) = \langle a, v(x) \rangle_{\mathbb{R}^d}$$

This will be denoted $M = \delta_x^*(a) \in \mathfrak{g}^*$.

iv. Differential operators: if $(f_{i,j}, 1 \le i, j \le d)$ are integrable functions, define

$$(M, v)=\sum_{i,j=1}^{d}\int_{\Omega} f_{ij}\frac{\partial v_i}{\partial x_j}dx$$

It is important to notice that, although L is defined in a rather abstract way in the previous lines, numerical procedures to compute geodesics can be derived most of the time from the knowledge of its inverse (of Green kernel) $K = L^{-1}$. This K is a smoothing kernel, the choice of which, within a specific range of available kernels, being the starting point of any practical procedure. We do not detail numerical algorithms in this paper, but the reader can refer to [4,5,17,23] for examples of choices of K.

2.2. Energy and Momenta

Consider a time-dependent diffeomorphism $v \in L^1([0, 1], \mathcal{g})$, and let (φ_{0t}^v, $t \in [0, 1]$) be the associated flow, defined in the previous section. Along time, each point $x \in \Omega$, considered as a particle, evolves on the trajectory $t \mapsto \varphi_{0t}^v(x)$, its velocity at time t being by definition $v_t(\varphi_{0t}^v(x))$. In other terms, for $y \in \Omega$, $v_t(y)$ is the instantaneous velocity of the particle which is at y at time t. It is called the Eulerian velocity at y at time t.

So, at each time, we have an Eulerian velocity field, $y \mapsto v_t(y)$, and we *define* the kinetic energy of the system to be $E(v_t)=\frac{1}{2}\|v_t\|_{\mathrm{g}}^2$. The total energy spent during the deformation path now is

$$E_{\mathrm{total}}(v)=\frac{1}{2}\int_0^1\|v_t\|_{\mathrm{g}}^2 dt.$$

Note that, in classical fluid mechanics, the kinetic energy is the sum of particle kinetic energies, which, for a homogeneous fluid with mass density given by ρ yields

$$\|v_t\|^2=\frac{\rho}{2}\int_{\Omega}|v_t(y)|^2 dy.$$

This is the L^2 norm of v, which cannot be used in our context, since we require that $\mathcal{g}$ is embedded in C_0^1 (we need some kind of Sobolev norms). However, in analogy with standard mechanical systems, we may define the global momentum of the system at time t to be the linear form $M_t \in \mathcal{g}^*$ such that $E(v_t) = (M_t, v_t)/2$, which, with the notation of the previous section, yields.

$$M_t=Lv_t.$$

So, if v_t is the Eulerian velocity field at time t, the momentum at time t is given by Lv_t. It will be called the momentum in Eulerian coordinates.

2.3. Lagrangian and Eulerian Frames

The Eulerian frame, as introduced above, describes mechanical quantities as they are observed in the current configuration at each time. The Lagrangian frame, on the contrary,

describes quantities as seen from the initial configuration. For example, the diffeomorphism $\varphi_{0t}^{v}(x)$ provides the position at time t of the particle which was at x at time 0, which is a Lagrangian notion. For the velocity, we create a Lagrangian velocity field by pulling back the previously defined velocity v_t, setting

$$v_t^l(x)=\frac{d}{ds}\left(\varphi_t^{-1}(\varphi_{t+s}(x))\right)_{|s=0},$$
$$\text{i.e.}\, v_t^l=(d\varphi_t)^{-1}(v_t\circ\varphi_t).$$

The operation

$$v\mapsto(d\varphi)v\circ\varphi^{-1}$$

defines a fundamental Lie group operation, and is called the adjoint action of G on its Lie algebra (which here is $\mathfrak{g}$), denoted $\mathrm{Ad}_\varphi v$. We have obtained the relation

$$v_t=Ad_{\varphi_t}v_t^l.$$

To interpret the adjoint action pictorially, the new vector field under the adjoint action $v\rightarrow(d\varphi)v\circ\varphi^{-1}$ has to be interpreted as the transformation of v under the deformation generated by φ. Figure 1 shows how the field v^l at location x is transported by the flow to the value $v(y)$ at location $y=\varphi(x)$ by pushing forward (using φ) the Lagrangian frame on which v^l is drawn. Note that the orientation of the vector $v(x)$ drawn on the deformed sheet is also changed (through the action of $(d\varphi)$).

2.4. Momentum in Eulerian and Lagrangian Coordinates

The momentum $M_t=Lv_t$, which has been defined in Eulerian coordinates, also admits a Lagrangian version. It can be computed by expressing the kinetic energy at time t, which is $(Lv_t, v_t)/2$, under the form $(M_t^l, v_t^l)/2$, M_t^l, being then the Lagrangian momentum. This is straightforward, since, by definition of an adjoint operator:

$$(Lv_t,v_t)=(Lv_t,Ad_{\varphi_t}v_t^l)=(Ad_{\varphi_t}^{*}Lv_t,v_t^l).$$

This leads to the definition $M_t^l=Ad_{\varphi_t}^{*}Lv_t$ for the momentum in Lagrangian coordinates. The Lagrangian frame takes here the role of a Galilean, or reference frame, and we will retrieve below the fundamental principle of mechanics, which states that the Lagrangian momentum is constant over time along any energy minimizing path. Before this, we make a brief interuption in our discussion to describe the relation between the classical mechanics of a rigid body, and geodesic equation in matrix Lie groups. This simple description will help to understand the formalism in our infinite dimensional group of diffeomorphisms.

3. Euler Equation and Conservation of the Momentum for Lie Groups of Matrices

In this part, we derive the Euler equation for extremal paths of the kinetic energy in the case of Lie groups of matrices. This derivation is well-known in the context of classical solid mechanics [1], but this simpler case, which can be derived completly without too much technicalities, may be helpful to understand the case of diffeomorphisms.

Let $G \subset \mathcal{M}_d(\mathbb{R})$ be a Lie group of $d \times d$ matrices with Lie algebra $\mathfrak{g}$. The case of interest is when G is a group of 3D rotations, which models the position of a rigid body with fixed center of mass. In this case, $\mathfrak{g}$ is the vector space of antisymmetric 3×3 matrices. Let $t \mapsto g_t$ be a trajectory in this group. Then, the angular velocity $a_t \in \mathfrak{g}$ is given by the equation $\frac{dg_t}{dt} = g_t a_t$. This is to be related to our previous definition of Eulerian velocity, which was

$$\frac{d\varphi_t}{dt} = v_t \circ \varphi_t$$

in which the (left) product of matrices is replaced by the (right) composition of functions.

Returning to the matrix case, we define the kinetic energy at time t to be $(Ja_t, a_t)/2$, for some symmetric positive definite operator $J: \mathfrak{g} \to \mathfrak{g}^*$. In the case of the rigid body, the angular velocity can be identified to a 3-vector ω_t, and J can be seen as a 3×3 matrix which only depends on the geometry of the object, called the inertia operator and, with some abuse of notation,

$$(Ja_t, a_t) = (J\omega_t, \omega_t).$$

(note that here the notation (,) refers to the sum of products of coordinates, i.e. the usual inner product on Euclidean spaces, after identification between $\mathfrak{g}$ and $\mathfrak{g}^*$). The total energy is

$$E(g) = \frac{1}{2}\int_0^1 (Ja_t, a_t)dt.$$

We retrieve again the analogy with the diffeomorphisms by letting

$$\langle a, b \rangle_g = (Ja, b)$$

so that J takes the role of L in the previous section.

We now compute the Euler equation for least energy paths between two fixed endpoints g_0 and g_1. We recall that the Lie bracket on $\mathfrak{g}$ is $[a, b] = ab - ba$.

Theorem 1

The Euler-Lagrange equation for the kinetic energy is given by

$$\frac{\partial Ja}{\partial t} - ad_a^*(Ja)=0. \tag{2}$$

where $ad_a^*:\mathrm{g}^* \rightarrow \mathrm{g}^*$ is defined by duality through the equalities $(ad_a^* f, b)=(f, ad_a b)=(f, [a, b])$.

Proof—Let $(t \mapsto g_0(t))$ be an extremal curve for the kinetic energy and $((t, h) \mapsto g(t, h))$ be a smooth deformation around $h = 0$ ($g(t, 0) = g_0(t)$): Let $a(t, h)$ and $A(t, h)$ be such that

$$\frac{\partial g}{\partial t}=ga \text{ and } \frac{\partial g}{\partial h}=gA. \tag{3}$$

Writing $\frac{\partial^2 g}{\partial t \partial h}=\frac{\partial^2 g}{\partial h \partial t}$, we get $gAa+g\frac{\partial a}{\partial h}=gaA+g\frac{\partial A}{\partial t}$ i.e.

$$\frac{\partial a}{\partial h}=\frac{\partial A}{\partial t}+[a, A]=\frac{\partial A}{\partial t}+\mathrm{ad}_a A. \tag{4}$$

The curve $A(t, h)$ can vary freely in $\mathfrak{g}$, with boundary conditions $A(0, h) = A(1, h) = 0$. From

$$\frac{d}{dh}\left(\int \langle a, a\rangle_{\mathrm{g}} dt\right)_{|h=0},$$

we get

$$\int \left\langle a, \frac{\partial A}{\partial t}+ad_a A\right\rangle_{\mathrm{g}} dt=\int \left(Ja, \frac{\partial A}{\partial t}+\mathrm{ad}_a A\right) dt=0 \tag{5}$$

Using the duality relation, we get $(Ja, \mathrm{ad}_a A)=(\mathrm{ad}_a^*(Ja), A)$ so that by integration by part, we finally obtain the Euler equation

$$\frac{\partial Ja}{\partial t} - \mathrm{ad}_a^*(Ja)=0. \tag{6}$$

We know from Lagrangian mechanics that the motion of a body with inertial operator J without external forces are extremal paths of the kinetic energy. Hence, Eq. (6) is the evolution equation of a body. We recognize in this equation the momentum to the body $M_t^b \doteq Ja_t$ and the Euler equation is then:

$$\frac{\partial M^b}{\partial t} - \mathrm{ad}_a^*(M^b)=0. \tag{7}$$

The momentum in the body here is to relate to the momentum in Eulerian coordinates for diffeomorphisms. However, if we study the motion of the body in a fixed static reference

frame, *the momentum to the space* denoted here M^s should remain constant in the absence of external forces. The momentum to the space is defined from $M^b{}_t$ by a change of reference frame:

$$M_t^b \doteq Ad^*_{g_t^{-1}}(M_t^b) \tag{8}$$

where Ad^*_g is the co-adjoint representation which is defined by duality through the equalities: $(\mathrm{Ad}^*_g f, b)=(f, \mathrm{Ad}_g b)=(f, gbg^{-1})$. We derive from the evolution equation for M^b, given by the Euler equation (7), the conservation of the momentum to the space M^s:

Theorem 2

Along extremal curves for the kinetic energy, M^s is constant:

$$\frac{dM^s}{dt}=0. \tag{9}$$

Proof—Indeed, we have

$$\left(\frac{dM_t^s}{dt}, b\right)=\frac{d}{dt}(M_t^s, b)=\frac{d}{dt}(Ja_t, \mathrm{Ad}_{g_t^{-1}} b)$$

Since, $\frac{d}{dt}(\mathrm{Ad}_{g_t^{-1}})= -\mathrm{ad}_{a_t}\mathrm{Ad}_{g_t^{-1}}$, we get finally using Euler Eq. (6),

$$\begin{aligned}\left(\tfrac{dM_t^s}{dt}, b\right) &= \left(\tfrac{\partial Ja}{\partial t} - \mathrm{ad}^*_a(Ja), \mathrm{Ad}_{g_t^{-1}} b\right)\\ &=0.\end{aligned} \tag{10}$$

Thus, from the conservation of the momentum to the space, $M_t^s \equiv M_0^s$, we deduce that

$$Ja_t=\mathrm{Ad}^*_{g_t}(La_0), \tag{11}$$

or equivalenty, for any $b \in \mathfrak{g}$:

$$(Ja_t, b)=(Ja_0, \mathrm{Ad}_{g_t} b) \tag{12}$$

These results are in fact true for any Lie-group with a left-invariant metric. As we now investigate, they can be formally extrapolated also for infinite dimensional groups of diffeomorphisms.

4. Geodesic Evolution of the Diffeomorphism and Conservation of Momentum

4.1. Euler Equation as Evolution Equation for the Momentum in Eulerian Coordinates

The derivation of the Euler equation for extremal paths of the kinetic energy in the case of finite-dimensional Lie groups can be carried out in full generality within the Lie theory framework, to lead to the law of conservation of momentum. A general computation can be found in [1]. In our infinite dimensional case, a rigorous derivation of this law is much harder, and must most of the time be obtained directly from variational and functional analysis arguments rather than with purely algebraic Lie group derivations. However, it is interesting, and quite informative, to use these derivations to obtain a formal proof of the conservation of momentum, without wondering too much about the well-posedness of the expressions. This will be done in the next paragraphs.

The first Euler equation provides the variations of the momentum in Eulerian coordinates. Before stating it, we need some definitions:

Definition 1—The adjoint action Ad of G on $\mathfrak{g}$ and the associated adjoint action ad of $\mathfrak{g}$ on itself are given with their dual operators Ad^*, ad^* by

$$\begin{aligned} \mathrm{Ad}_\varphi w &= (d\varphi) w \circ \varphi^{-1}, \\ (\mathrm{Ad}^*_\varphi f, w) &= (f, \mathrm{Ad}_\varphi w) \end{aligned} \tag{13}$$

$$\begin{aligned} \mathrm{ad}_v w &= [v, w] = (dv)w - (dw)v, \\ (\mathrm{ad}^*_v f, w) &= (f, \mathrm{ad}_v w). \end{aligned} \tag{14}$$

with $\varphi \in G$, $w \in \mathfrak{g}$, $f \in \mathfrak{g}^*$.

Already at this point, one can point out the difficulty of the infinite dimensional problem: at the difference with the matrix case, if v, w belong to $\mathfrak{g}$, it cannot be guaranteed that it is still so for $[w, v] = (dw)v - (dv)w$: in situations of interest, $\mathfrak{g}$ is, in fact, not a Lie algebra: $\mathrm{Ad}_\varphi w$ and $\mathrm{ad}_v w$ do not necessarily belong to $\mathfrak{g}$. As a consequence, the definition of $\mathrm{ad}^*_v f$ which has been given cannot hold without some restriction on f, in order to be able to extend it to vector fields which are brackets of elements of $\mathfrak{g}$. We however proceed with such formal computation without addressing these issues.

The geodesics are extremal curves for the kinetic energy. They satisfy an Euler equation giving the variation of the momentum in terms of the co-adjoint action operator on the momentum.

Statement 1—The Euler equation for the kinetic energy is given by

$$\frac{dLv}{dt} + ad^*_v(Lv) = 0. \tag{15}$$

When $Lv \in H$ (i.e. it is a function), one has

$$\mathrm{ad}_v^* Lv = \mathrm{div}(Lv \otimes v) + dv^* Lv. \tag{16}$$

where $\mathrm{div}(u \otimes v) = duv + \mathrm{div}(v)u$.

These equations, which are derived below, are special cases of the Euler-Poincaré principle, described, for example in [19]. Equation (15) is formally identical to Eq. (2) in the matrix case, excepted for a sign difference arising from the switch from a left-invariance in the matrix case to a right-invariance in the diffeomorphism case.

Formal Justification—This is exactly as in the matrix case. Here again, let $(t \mapsto \varphi_t)$ be extremal and $((t, \varepsilon) \mapsto \varphi_{t,\varepsilon})$ be a smooth deformation around $\varepsilon = 0$, with the abuse of notation $\varphi_{t,0} = \varphi_t$. Denote $\frac{\partial \varphi_{t,\varepsilon}}{\partial t} = v_{t,\varepsilon} \circ \varphi_{t,\varepsilon}$, $\frac{\partial \varphi_{t,\varepsilon}}{\partial \varepsilon} = \eta_{t,\varepsilon} \circ \varphi_{t,\varepsilon}$, $\frac{\partial v_{t,\varepsilon}}{\partial \varepsilon} = h_{t,\varepsilon}$, still denoting $v_{t,0} = v_t$, $\eta_{t,0} = \eta_t$ and $h_{t,0} = h_t$. Our first step is to express h_t in function of the other variables. For this, write

$$\frac{\partial^2 \varphi}{\partial \varepsilon \partial t} = \frac{\partial^2 \varphi}{\partial t \partial \varepsilon}$$

which yields

$$h_t \circ \varphi_t + d_{\varphi_t} v_t \eta_t \circ \varphi_t = \frac{\partial \eta_t}{\partial t} \circ \varphi_t + d_{\varphi t} \eta_t v_t \circ \varphi_t$$

or (applying φ_t^{-1} on the right to both terms) gives

$$h_t = \frac{\partial \eta_t}{\partial t} + d\eta_t v_t - dv_t \eta_t = \frac{\partial \eta_t}{\partial t} + [\eta_t, v_t].$$

The[1] first variation of the energy is given by

$$\begin{aligned} &\tfrac{d}{d\varepsilon} \int_0^1 \|v_{t,\varepsilon}\|_g^2 dt \\ &= 2 \int_0^1 \langle v_t, h_t \rangle_g dt \\ &= \int_0^1 \left\langle v_t, \tfrac{d\eta_t}{dt} + [\eta_t, v_t] \right\rangle_g dt \\ &= \int_0^1 \left(Lv_t, \tfrac{d\eta_t}{dt} \right) dt - \int_0^1 (Lv_t, ad_{v_t} \eta_t) dt. \end{aligned}$$

Since φ_t is extremal, this expression vanishes for all η (with $\eta_0 = \eta_1 = 0$), and a last integration by parts yields

[1]These arguments are purely formal since h_t includes the Lie bracket which cannot be guaranteed to belong to $\mathfrak{g}$ (in which case our variation would not be justified).

$$\frac{dLv_t}{dt}+ad^*_{v_t}Lv_t=0,$$

which is Eq. (15).

We now prove Eq. (16) under the assumption that Lv is a function. By definition

$$\begin{aligned}(ad^*_vLv,w)&=(Lv,dvw-dwv)\\&=(dv^*Lv,w)-(Lv,dwv)\end{aligned}$$

and the conclusion comes from Stokes' theorem which states that (since v and w vanish on $\partial\Omega$)

$$(\mathrm{div}(Lv\otimes v),w)=-(Lv,dw.v).$$

It appears that the Euler equation (15) with $\mathrm{ad}^*_vLv=\mathrm{div}\,vLv+dv^*Lv$ has been derived in [26] and subsequently [22] directly as the Euler-Lagrange equation for the kinetic energy by analytical means. This has been originally proved by Arnold in [3] for the motion of impressible fluid which corresponds to the case L = Id with the constraint div v = 0.

4.2. Conservation of Momentum in Lagrangian Coordinates

The Euler equation (15) is the evolution of the momentum in Eulerian coordinates. We recognize in this equation the momentum $M_t \doteq Lv_t$; the momentum in Eulerian coordinates evolves in time so as to balance the co-adjoint of the momentum thereby satisfying the associated Euler equation $\frac{dM_t}{dt}+ad^*_{v_t}(M_t)=0$ for extremal paths. However, *the momentum in Lagrangian coordinates*, identified in the introduction as $M^l_t=\mathrm{Ad}^*_{\varphi_t}(M_t)$, remains constant in the absence of external forces, $\frac{d}{dt}M^l_t=0$.

Statement 2—Along extremal curves for the kinetic energy, M^l_t is constant:

$$\frac{dM^l_t}{dt}=0. \tag{17}$$

In particular, we have for all $w\in\mathfrak{g}$,

$$(Lv_t,w)=(Lv_0,(d\varphi_t)^{-1}w\circ\varphi_t). \tag{18}$$

Formal Derivation—Indeed, fix $w\in\mathfrak{g}$ and let $f(\varepsilon)=(M^l_{t+\varepsilon},w)$. We have, on the first hand $f'(0)=(\frac{dM^l_t}{dt},w)$, and on the second hand (derivatives being evaluated at time ε = 0)

$$f'(0)=\frac{d}{d\varepsilon}(Lv_{t+\varepsilon},\mathrm{Ad}_{\varphi_{t+\varepsilon}}w)$$
$$=\left(\frac{dLv_t}{dt},\mathrm{Ad}_{\varphi_t}w\right)+\left(Lv_t,\frac{d}{d\varepsilon}Ad_{\varphi_{t+\varepsilon}}w\right)$$

Note here that $\mathrm{Ad}_{\varphi\circ\varphi'}=\mathrm{Ad}_{\varphi}\,\mathrm{Ad}_{\varphi'}$. Now, if $\varphi_0=\mathrm{id}$ and $\frac{d\varphi_\varepsilon}{d\varepsilon}=v$ at $\varepsilon=0$, we have for any w',

$$\frac{d}{d\varepsilon}(\mathrm{Ad}_{\varphi_\varepsilon}w')|_{\varepsilon=0}=\frac{d}{d\varepsilon}\left((d\varphi_\varepsilon)w'\circ\varphi_\varepsilon^{-1}\right)|_{\varepsilon=0}$$
$$=dv(w')-dw'(v)=ad_vw'. \tag{19}$$

Applying this to $w'=\mathrm{Ad}_{\varphi_{t-1}}$ and $v=v_t$, we get

$$f'(0)=\left(\frac{dLv_t}{dt},\mathrm{Ad}_{\varphi_t}w\right)+(Lv_t,ad_{v_t}Ad_{\varphi_t}w)$$
$$=\left(\frac{dLv_t}{dt}+ad^*_{v_t},Ad_{\varphi_t}w\right)=0$$

by Eq. (15). This completes the proof,

$$\left(\frac{dM_t^l}{dt},w\right)=0.$$

Although the conservation of momentum has only been derived from formal arguments, we can check that, when it is satisfied, the generated deformation paths do provide extremal curves of the kinetic energy. The perturbation of the end point of the path (φ^v_{0t}, $t\in[0,1]$) at time 1 under a perturbation v_t^ε of v_t is given by [22]:

$$\frac{d}{d\varepsilon}\varphi^{v^\varepsilon}_{01}(x)=\int_0^1 d_{\varphi^v_{0s}}\varphi^v_{s1}(h_s\circ\varphi^v_{0s})ds. \tag{20}$$

with $h_s(x)=\frac{dv_s^\varepsilon(x)}{d\varepsilon}$, the derivative being taken at $\varepsilon=0$ (we have used the notation of Eq. (1)). Assume that this expression vanishes (so that the end point $\varphi^{v^\varepsilon}_{01}$ remains unchanged). The first variation of the kinetic energy is given by $\int_0^1\langle v_t,h_t\rangle_L dt=\int_0^1(Lv_t,h_t)dt=\int_0^1(Lv_0,d_{\varphi_{0t}}\varphi_{t0}v_t\circ\varphi_{0t})dt$. Now, using (20) and the fact that $d_{\varphi 0t}\,\varphi_{t1}=d_{\varphi 00}\,\varphi_{01}d_{\varphi 0t}\,\varphi_{t0}$, we get easily that $\int_0^1 d_{\varphi_{0t}}\varphi_{t0}v_t\circ\varphi_{0t}dt=0$ so that, by linearity,

$$\int_0^1\langle v_t,h_t\rangle_L dt=\left(Lv_0,\int_0^1 d_{\varphi_{0t}}\varphi_{t0}h_t\circ\varphi_{0t}dt\right)=0. \tag{21}$$

4.3. Coadjoint Transport of Structures Along a Geodesic

For $M\in\mathfrak{g}^*$, the evolution $t\mapsto\mathrm{Ad}^*_{\varphi_t^{-1}}M$ is called coadjoint transport. The fact that the momentum evolves by coadjoint transport along a geodesic implies the conservation of

several properties whenever they are initially true, for Lv_0. These properties will turn out to be of main importance for image processing applications.

In this section, we assume that $M_0 = Lv_0$ is given, and that the coadjoint transport $M_t = Lv_t = Ad^*_{\varphi_{t0}}(M_0)$ is well defined at all considered times.

4.3.1. Coadjoint Evolution of the Support—Let Supp(M) denote the support of a momentum $M \in \mathfrak{g}^*$. It is defined by the complementary of the union of all open sets $\Omega' \subset \Omega$ which are such that $(M, w) = 0$ whenever $w \in \mathfrak{g}$ vanishes outside Ω'. We have the property:

Statement 3: If $M_t = \mathrm{Ad}^*_{\varphi_{t0}}(M_0)$, then

$$\mathrm{Supp}(M_t) = \varphi^v_{0t}(\mathrm{Supp}(M_0))$$

Indeed, assume that M_0 vanishes $\Omega' \subset \Omega$. Let w have its support included in $\varphi_{0t}(\Omega')$. Then $(M_t, w) = (M_0, d\varphi_{0t})^{-1}\, w \circ \varphi_{0t}$ and $w \circ \varphi_{0t}$ vanishes outside Ω', which implies that $(M_t, w) = 0$. Thus $\mathrm{Supp}(M_t) \subset \varphi_{0t}(\mathrm{Supp}(M_0))$, and the reverse inclusion is true by inverting the roles of M_0 and M_t.

As a first example, consider the case when M_0 is finitely supported, and more precisely a sum of Dirac measures. This is legitimate since our hypotheses on L imply that Dirac measures belong to $\mathfrak{g}^*$, therefore have the form Lv_0 for some $v_0 \in \mathfrak{g}$. So, we assume that

$$(M_0, w) = \sum_i \langle a_i, w(x_i) \rangle_{\mathbb{R}^d}, \tag{22}$$

where $(x_i)_{1 \le i \le n}$ is a finite family of points in Ω (landmarks) and $(a_i)_{1 \le i \le n}$ is a finite family of vectors in $\mathbb{R}^d$. We write $M_0 = \sum_{i=1}^n \delta^*_{x_i} a_i$, where, by definition

$$\begin{aligned} \delta^*_x a : \mathfrak{g} &\to \mathbb{R} \\ w &\mapsto \langle a, w(x) \rangle \end{aligned} \tag{23}$$

Denoting $x_i(t) \doteq \varphi_t(x_i)$, we obtain the fact that M_t is supported on $\{x_1(t), \ldots, x_N(t)\}$. More precisely, a rapid computation shows that

$$M_t = \sum_{i=1}^n \delta^*_{x_i(t)} a_i(t) \tag{24}$$

with

$$a_i(t) = (d_{x_i(t)} \varphi_{t0})^* a_i \tag{25}$$

so that the momentum remains a sum of Dirac measures. This is a special case of the property considered in the next section.

4.3.2. Coadjoint Transport of Measure—Measure-based momenta are given by

$$(M, w)=\int_{\Omega}\langle v_0, w\rangle d\mu_0 \tag{26}$$

where μ_0 is a measure on Ω and v_0 is measurable and μ_0-integrable. They generate a large class of geodesic evolutions, and have the attractive property that the momentum Lv_t can be explicitly computed from the momentum at the origin.

Statement 4: Assume that $(M_0, w) = \int_{\Omega}\langle v_0, w\rangle d\mu_0$ then the linear momentum functional evolves according to

$$\begin{aligned}(M_t, w)&=\int_{\Omega}\langle v_t, w\rangle_{\mathbb{R}^d} d\mu_t \quad \text{where}\\ v_t(x)&=(d_x\varphi_{t0})^{*}v_0\circ\varphi_{t0}(x), \mu_t \doteq \mu\circ\varphi_{t0},\end{aligned} \tag{27}$$

i.e. $\mu_t(A) = \mu(\varphi_{t0}(A))$ for any measurable set A.

The statement follows straightforwardly from the substitutions

$$\begin{aligned}(M_t, w)&=\int_{\Omega}\left\langle v_0(x), ((d\varphi_{0t})^{-1}w\circ\varphi_{0t})(x)\right\rangle_{\mathbb{R}^d} d\mu(x)\\ &=\int_{\Omega}\left\langle d_{\varphi_{0t}}(x)\varphi_{t0}^{*}v_0(x), w\circ\varphi_{0t}(x)\right\rangle_{\mathbb{R}^d} d\mu_0(x)\\ &=\int_{\Omega}\langle v_t(x), w(x)\rangle_{\mathbb{R}^d} d\mu_t(x)\end{aligned} \tag{28}$$

Point-supported momentum evolution considered in the previous section, clearly is a particular case of this statement. As another illustration, consider the case of measures which are supported by submanifolds of Ω. In this case, the initial momentum is concentrated along the boundary Σ_0 of a k-dimensional C^1 sub-manifold in $\Omega \subset \mathbb{R}^d$.

Let σ_0 by the surface measure (given as the induced volume form on the sub-manifold) and let μ_0 be supported by Σ_0, such that for any smooth function on Ω, $\int_{\Omega} f\, d\mu_0 = \int_{\Sigma_0} f\,\alpha_0 d\sigma_0$ for some density α_0 (not necessary positive) on the surface. Let v_0: $\Omega \to \mathbb{R}^d$ (the values of v_0 outside Σ_0 will not be important) and define

$$(Lv_0, w)=\int_{\Sigma_0}\langle v_0, w\rangle_{\mathbb{R}^d}\alpha_0 d\sigma_0. \tag{29}$$

Using Statements 3 and 4, we get that the tranported measure μ_t is located on the transported sub-manifold $\Sigma_t \doteq \varphi_t(\Sigma_0)$ (whose smoothness is preserved by the regularity of the diffeomorphisms in G) and can be written as $\mu_t = \alpha_t\,\sigma_t$ where σ_t is the k-dimensional volume measure on Σ_t. Moreover, if $v_t = d(\varphi_{t0})^{*}\gamma_0\circ\varphi_{t0}$, Statement 4 gives us the evolution of the momentum

$$(Lv_t, w) = \int_{\Sigma_t} \langle v_t, w \rangle \, \alpha_t d\sigma_t(y). \tag{30}$$

In the case where the sub-manifold is Ω itself, then $\sigma_t = \sigma_0$ is the Lebesgue's measure λ on Ω, and $\alpha_t = \alpha_0 \circ \varphi_{t,0} |d\varphi_{t,0}|$.

4.3.3. Coadjoint Transport of Orthogonality—The last property transported by geodesic evolution which is considered here is the normality with respect to a smooth submanifold of Ω. Since normality will be extensively studied in the next section, we here provide an illustration in a particular case.

Assume that v_0, in Eq. (26) can be expressed as

$$v_0 = \sum_{i=1}^{r} b_0^i \nabla f_0^i \tag{31}$$

where $(b_0^i)_{1 \le i \le r}$ and (f_0^i) are two families of functions on Ω and $1 \le r \le d$. Then, we get from Statement 4 that

$$v_t = \sum_{i=1}^{r} b_t^i \nabla f_t^i \tag{32}$$

where $b_t^i = b_0^i \circ \varphi_{t,0}$ and $f_t^i = f_0^i \circ \varphi_{t,0}$. Equation (32) can be interpreted as a normality property of the geodesic motion under initial condition (31). Indeed, let

$$\sum\nolimits_0 = \bigcap_{i=1}^{r} (f_0^i)^{-1}(\{0\}).$$

Assume that Σ_0 is not empty and denotes $N_0(x) = \mathrm{Span}\{\nabla f_0^i(x) | 1 \le i \le r\}$ for any $x \in \Sigma_0$. Under appropriate transversality conditions, mainly

$$r \equiv \dim N_0,$$

Σ_0 can be equipped with a structure of $(d - r)$-dimensional C^1 manifold and $N_0(x)$ is exactly the space of vectors normal to Σ at location x.

We then deduce easily that

$$\sum\nolimits_t = \bigcap_{i=1}^{r} (f_t^i)^{-1}(\{0\})$$

and equality (32) implies for any $x \in \Sigma_t$

$$\nu_t(x) \in N_t(x) \tag{33}$$

where $N_t(x)=\text{Span}\{\nabla f_t^i(x) | 1 \leq i \leq r\}$ is the set of normal vectors to Σ_t at location x.

We deduce that if the momentum is normal to some k-dimensional sub-manifold Σ_0, this normality property is preserved by coadjoint transport along a geodesic.

In the case of $r = 1$ and $f_0^1=f_0$, Σ_0 is exactly the level set for threshold value 0 of f_0 and the normality of the initial momentum to the level sets is preserved under geodesic motion. Since the threshold value is arbitrary, we deduce that the property is true for all level sets.

5. The Normal Momentum Motion Constraint

5.1. Heuristic Analysis

The conservation of momentum is a general property of geodesics in a group of diffeomorphisms with a right invariant metric. More can be said in the situation when diffeomorphisms are associated to deformations of geometric structures or images, which is the situation of interest for our applications. In this setting we are still looking for curves with shortest length in G, but we partially relax the fixed end-point condition by the constraint that the initial template is correctly mapped to the target: because there is a whole range of diffeomorphisms which deform one given structure into another, this condition is weaker than the fixed end-point condition, which means that there are more degrees of freedom for the optimization, and therefore more constraints on the minimum. For image matching, these additional constraints may essentially be summarized by the statement *the momentum along the geodesic path is at all times normal to the level sets of the image*. This is what we call the *normal momentum constraint*, which is described in this section.

We start with a heuristic analysis, for which I_0, the image, is a smooth function defined on Ω. Let I_1 be in the orbit of I_0 for the group G of diffeomorphisms: there exists $\psi \in G$ such that $I_0 \circ \psi^{-1} = I_t$. By compactness and semi-continuity arguments, one can prove the existence of a geodesic path $\varphi = (\varphi_t)$ such that

$$d_G(\text{Id}, \varphi_1)=\inf_{\phi \in G} d_G(\text{Id}, \phi) \text{ and } I_0=I_1 \circ \phi. \tag{34}$$

Let $\varphi=(\varphi_t^v)$ be such a solution and consider a first order expansion around $t = 0$, $\varphi_t(x) \simeq x + tv_0(x)$ so that $I_t=I_0 \circ \varphi_t^{-1}(x) \simeq I_0 - t\langle \nabla I_0, v_0 \rangle_{\mathbb{R}^d}$. By definition, the cost to go from I_0 to I_t is (still at first order) $t|v_0|_L$. However, any $u \in \mathfrak{g}$ such that $\langle \nabla I_0, u \rangle_{\mathbb{R}^d} = \langle \nabla I_0, v_0 \rangle_{\mathbb{R}^d}$, will lead to the same I_t so that the least deformation cost from I_0 to I_t should be $t|p_{I_0}(v_0)|$ where $p_{I_0}(v_0)$ the unique solution of the minimization problem:

$$\begin{aligned} &(\mathcal{P}_0): \inf_{u \in \mathfrak{g}} |u|_L \text{ subject to:} \\ &\langle (v_0 - u)(x), \quad \nabla I_0(x) \rangle_{\mathbb{R}^d} = 0, \quad \forall x \in \Omega \end{aligned} \tag{35}$$

Since (φ_t^v) is a geodesic path minimizing the deformation cost from I_0 to I_1, it minimizes also the deformation cost from I_0 to I_t yielding

$$v_0 = p_{I_0}(v_0). \tag{36}$$

Introduce the set $\mathfrak{g}_{I_0} = \{h \in \mathfrak{g} \mid \langle \nabla I_0(x), h(x) \rangle_{\mathbb{R}^d} = 0, \forall x \in \Omega\}$: the constraints in $\mathcal{P}_0$ can be restated as $u - v_0 \in \mathfrak{g}_{I_0}$ so that $p_{I0}(v)$ is the orthogonal projection of v on $\mathfrak{g}_{I_0}^{\perp}$, the space orthogonal to $\mathfrak{g}_{I_0}$. Hence, equality (36), translates to

$$\begin{aligned} &\forall h \in \mathfrak{g} \text{ such that for all } x \in \Omega, \langle \nabla I_0(x), h(x) \rangle = 0, \\ &\qquad \text{we have } \langle v_0, h \rangle_L = 0. \end{aligned} \tag{37}$$

Now, the fact that $\langle \nabla I_0(x), h(x) \rangle \equiv 0$ means that h is a vector field which is tangent to the level sets of I_0, and since $\langle v_0, h \rangle_L = (Lv_0, h)$, we see that Lv_0 vanishes when applied to any such vector field, or, that Lv_0 is a linear form which is normal to the level sets of I_0.

5.2. Rigorous Result

We now pass to a rigorous derivation of this property. Since it will be interesting to also consider images which are not smooth, we provide a new definition of the set $\mathfrak{g}_{I_0}$. Obviously, when I_0 is smooth, $h \in \mathfrak{g}_{I_0}$ is equivalent to the fact that, for any function f which is C^1 on Ω, one has

$$\int_\Omega \langle \nabla_x I_0, h(x) \rangle_{\mathbb{R}^k} f(x) dx = 0.$$

Applying the divergence theorem (we assume that $\partial\Omega$ is smooth enough and take advantage on the fact that elements of $\mathfrak{g}$ vanish on $\partial\Omega$), we get

$$-\int_\Omega I_0(x) \mathrm{div}(hf)(x) dx = 0.$$

Since this has a meaning when $I_0 \in L^2(\Omega)$, we now define

Definition 2—When $I \in L^2(\Omega)$, we denote

$$\mathfrak{g}_I = \{h \in \mathfrak{g} : \langle I, \ \mathrm{div}(hf) \rangle_{L^2} = 0 \text{ for all } f \in C^1(\Omega)\}.$$

We still denote by p_I the orthogonal projection on $\mathfrak{g}_I^{\perp}$. The group G is assumed to be built as described in Section 2.1 (in particular $\mathfrak{g}$ is continuously embedded in $C^1(\Omega, \mathbb{R}^d)$).

Theorem 3. (Normal Momentum Constraint): Assume that $I_0 \in L^2(\Omega)$ and let $\varphi = (\varphi_t^v)$ be a geodesic path solution of (34). Then, for almost all $t \in [0, 1]$

$$v_t \in \mathfrak{g}_{I_t}^{\perp}.$$

The proof is given in Appendix A.

5.3. Examples

Consider again the case of smooth I, so that the condition $h \in \mathfrak{g}_I$ is equivalent to $h \in \mathfrak{g}$ and for all $x \in \Omega$, $\langle \nabla_x I, h(x) \rangle_{\mathbb{R}^d} = 0$. Using notation (23), we get that $\langle \nabla I_0(x), h(x) \rangle_{\mathbb{R}^d} = \langle \delta_x^*(\nabla I_0(x)), h \rangle_L$ so that $\mathfrak{g}_{I_0} = (\mathrm{Span}\{\delta_x^*(\nabla I_0(x)) | x \in \Omega\})^\perp$ and finally,

$$\mathfrak{g}_I^\perp = \overline{\mathrm{Span}\{\delta_x^*(\nabla I(x)) | x \in \Omega\}}. \tag{38}$$

Vector fields v such that

$$(Lv, u) = \int_\Omega \langle v(x), u(x) \rangle_{\mathbb{R}^d} d\mu(x), \tag{39}$$

where v is normal[2] to the level sets of I belong to $\mathfrak{g}_I^\perp$ and it can be shown that they form a dense subset.

For non-smooth I, we can similarly introduce $\omega_f(I)$, as the unique element of $\mathfrak{g}$ such that, for $h \in V$, $\langle \omega_f(I), h \rangle = \langle I, \mathrm{div}(h f) \rangle_{L^2(\Omega)}$, and conclude that

$$\mathfrak{g}_I^\perp = \overline{\mathrm{Span}\{\omega_f(I) | f \in C^1(\Omega, \mathbb{R})\}}. \tag{40}$$

This implies that any element $v \in \mathfrak{g}_I$ is such that Lv can be expressed as a limit

$$(Lv, u) = \lim_{N \to \infty} \int_\Omega I(x) \mathrm{div}(u f_N)(x) dx$$

where $f_N \in C^1(\Omega, \mathbb{R})$. The particular case when I is the indicator function of a smooth domain $B \subset \Omega$ (which can be interpreted as a smooth shape) is quite interesting. For $x \in \partial B$, let $\nu(x)$ be the outward normal to $\partial\Omega$ and denote σ_B be the uniform measure on ∂B. Then

$$\begin{aligned} \int_\Omega I(x) \mathrm{div}(uf)(x) dx &= \int_B \mathrm{div}(uf)(x) dx \\ &= \int_{\partial B} f(x) \langle u(x), \nu(x) \rangle_{\mathbb{R}^d} d\sigma_B(x). \end{aligned}$$

In this case, we obtain a dense subspace of $\mathfrak{g}_I$ by considering elements $v \in \mathfrak{g}$ such that

$$(Lv, u) = \int_{\partial B} \langle v(x), u(x) \rangle_{\mathbb{R}^d} d\mu(x). \tag{41}$$

for some measure μ on ∂B (the boundary of the shape).

[2]When I has smooth level sets, we say that a vector field v is normal to its level sets when, denoting by Ω_i the set $\{I \leq i\}$, $v(x)$ is normal to $\partial \Omega_i$ if $x \in \partial\Omega_i$ for some i and $x = 0$ otherwise.

Remark—We close this section with a technical, but important, remark. We have called *normal momentum constraint* the property that $v_t \perp \mathcal{g}_{I_t}$ at almost all times. We have shown that this property is always true for geodesics minimizing (34). But there is another important issue, which is how much it constrains v_t, or, in other terms, how big $\mathcal{g}_I$ is for a given image I. That this is relevant, and sometimes non-trivial, may be seen from the following example: assume that we are in 2 dimensions ($d = 2$) and that I is a C^1 image, with a non-vanishing gradient, at least on a dense subset of Ω. Then, on any point x such that $\nabla_x I \neq = 0$, we can de-fine in a unique way a positively oriented orthonormal frame $(\tau(x)\ v(x))$ such that $v(x) = \nabla_x I/|\nabla_x I|$. Then, if $h \in \mathcal{g}_I$ and $h(x) \neq = 0$, we must have $h/|h| = \pm\tau$ in a small ball around x. Now h, as an element of $\mathcal{g}$ must be smooth (depending on the choice made for L, and $h/|h|$ has the same smoothness as h: this is impossible to achieve when τ itself is not smooth enough, which in such a case forces $h(x) = 0$. We thus get the property that h vanishes whenever $\tau(x)$ does not meet the smoothness requirements of $\mathcal{g}$, which may very well be everywhere on Ω (or on a dense subset, which is the same since h is continous), in which case $\mathcal{g}_I = \{0\}$ and the constraint is void, contrary to our intuition that the momentum should be aligned with v. We see that, for the constraint to really be effective, we need some smoothness requirement on I. Fortunately, as illustrated by the example above, this smoothness is only required for the *level sets* of I, which must have a smooth boundary. With such an assumption, for example, one can show that if $v \perp \mathcal{g}_I$ and

$$(Lv, u) = \int_\Omega \langle \xi(x), u(x) \rangle\, d\mu(x)$$

for some measure μ on Ω and some vector field on $\xi\ \Omega$, then ξ must be (μ-almost everywhere) orthogonal to the level sets of I. From a practical point of view smoothness of level sets may easily be obtained using algorithms such as mean curvature motion ([27]).

5.4. Conservation and Normality Property Check for Inexact Matching

Here, we give a brief account of situations in which proofs of conservation of momentum and the normality property can be carried on in a well-defined context, and retrieve the evolutions described in the previous section.

It is hard to make rigorous, in full generality, the variational argument we have used in the proof of Eq. (15). Notice that the well-definiteness of the conservation of momentum Eq. (17) is an issue by itself, since, when $w \in \mathcal{g}$, and φ_t is the diffeomorphism generated by a geodesic, there is a priori no reason for $(d\varphi_t)^{-1} w \circ \varphi_t)$ to belong to $\mathcal{g}$: one must be able to define Lv_0 on spaces which are bigger than $\mathcal{g}$, which means that Lv_0 needs to be somewhat smoother (as a distribution) than a generic element of $\mathcal{g}^*$.

However, there is a setting in which such a fact is true and easy to obtain: it is when the search for the geodesic is done with an approximation of the target, with some L^2 penalty term added to control the error. We summarize this setting in the case of landmark matching, shape matching and image matching. In these three situations, we will retrieve the coadjoint transport of measure-based momenta. In all cases, results in [11,35] ensure the existence of minimizers of the variational problem.

5.4.1. Inexact Landmark Matching—In this section, we assume that a measured space $(\mathcal{J}, \rho)$, together with two measurable functions x, y: $\mathcal{J} \to \Omega$ are given. The diffeomorphism φ is searched to minimize

$$U(\varphi)=E(\varphi)+\frac{1}{\sigma^2}\int_{\mathcal{J}}|y_i-\varphi(x_i)|^2 d\rho(i)$$

When ρ is discrete, this relates to point-based matching, x representing the landmark original positions and y giving the landmark target positions. If we express U in function of v, this requires the minimization of

$$\tilde{U}(v)=\int_0^1 \|v_t\|_L^2 dt+\frac{1}{\sigma^2}\int_{\mathcal{J}}|y_i-\varphi_{01}^v(x_i)|^2 d\rho(i)$$

The main point here is to notice that the optimal solution v generates a geodesic in G between id and φ_1^v.

Proposition 1: Denote $\delta_x^* a$ the linear form on $\mathcal{g}$ such that $(\delta_x^* a, v)=\langle a, v(x)\rangle$. Let v be a minimizer of $\tilde{U}$. Then, letting $x_i(t)=\varphi_{0t}^v(x_i)$

$$Lv_t=-\frac{1}{\sigma^2}\int_{\mathcal{J}}\delta_{x_i(t)}^*[(d_{x_i(t)}\varphi_{t1}^v)^*(y_i-x_i(1))]d\rho(i) \tag{42}$$

Proof: The proof of this result is a direct consequence of the identity, valid for $s, t\in[0,1]$, $v, h\in L^2([0,1],\mathcal{g})$,

$$\frac{d}{d\varepsilon}\varphi_{st}^{v+\varepsilon h}(x)\Big|_{\varepsilon=0}=\int_s^t d_{\varphi_{su}^v}\varphi_{ut}^v(h_u\circ\varphi_{su}^v)du. \tag{43}$$

the proof of which being carried on with usual ODE arguments and being omitted here. It is then straightforward to obtain (42), using the definition of the linear forms $\delta_x^* a$, for $x\in\Omega$ and $a\in\mathbb{R}^d$.

Equation (42) is a conservation of momentum equation for

$$Lv_0=-\frac{1}{\sigma^2}\int_{\mathcal{J}}\delta_{x_i}^*[(d_{x_i}\varphi_{01}^v)^*(y_i-x_i(1))]d\rho(i).$$

When $\mathcal{J}$ is finite, this is equation (31) with $a_i=-\frac{1}{\sigma^2}(d_{x_i}\varphi_{01}^v)^*(y_i-x_i(1))$. Equation (42) now is exactly (24), since

$$\begin{aligned} a_i(t)&=(d_{x_i(t)}\varphi_{t0}^v)^* a_i\\ &=-\tfrac{1}{\sigma^2}[d_{x_i(0)}\varphi_{01}^v d_{x_i(t)}\varphi_{t,0}^v]^*(y_i-x_i(1))\\ &=-\tfrac{1}{\sigma^2}(d_{x_i(t)}\varphi_{t1}^v)^*(y_i-x_i(1)) \end{aligned}$$

5.4.2. Inexact Shape Matching—We now consider the comparison of a binary set-indicator function, $I_0 = \mathbf{1}_{\Omega_0}$ ($\bar{\Omega}_0 \subset \Omega$ having smooth boundaries) and a smooth function I_1, through the minimization of

$$U(\varphi)=E(\varphi)+\frac{1}{\sigma^2}\int_\Omega |\mathbf{1}_{\Omega_0}\circ\varphi^{-1}(x)-I_1(x)|^2dx$$

over G_L. We have

Proposition 2: Let v be a minimizer of $U(\varphi_{01}^v)$ over $L^2([0,1],\mathcal{g})$. Then

$$Lv_t=\frac{1}{\sigma^2}\int_{\partial\Omega_1}\left(\frac{1}{2}-I_1\right)\delta^*_{\varphi^v_{1t}(x)}[(d_{\varphi^v_{1t}}\varphi^v_{t1})^*\nu_1]d\sigma_1(x) \tag{44}$$

where $\Omega_1=\varphi^v_{01}(\Omega_0)$, ν_1 is the outward normal to $\partial\,\Omega_1$ and σ_1 is the volume measure on $\partial\,\Omega_1$.

Proof: Taking a variation $v + \varepsilon h$, the main issue is to compute the derivative of

$$\frac{1}{2}\int_\Omega |\mathbf{1}_{\Omega_0}\circ\varphi_{10}^{v+\varepsilon h}(x)-I_1(x)|^2dx$$

This integral can be rewritten

$$\int_{\Omega_{01}^{v+\varepsilon h}(\Omega_0)}\left(\frac{1}{2}-I_1(x)\right)dx+\frac{1}{2}\int_\Omega |I_1(x)|^2dx$$

Since the last term is constant, we see that the problem boils down to the computation of the derivative of the first term, which can be written, after a change of variable and letting $f_1 = 1/2 - I_1$,

$$\int_{\Omega_0} f_1\circ\varphi_{01}^{v+\varepsilon h}(x)|d_x\varphi_{01}^{v+\varepsilon h}|dx$$

Define u by $u\circ\varphi^v_{01}(x)=\frac{d}{d\varepsilon}\varphi_{01}^{v+\varepsilon h}(x)$. Simple computations, which can be, for example, found in [10], yields the fact that

$$\frac{d}{d\varepsilon}\int_{\Omega_0} f_1\circ\varphi_{01}^{v+\varepsilon h}(x)|d_x\varphi_{01}^{v+\varepsilon h}|dx=\int_{\Omega_1}\mathrm{div}(f_1u)dx$$

Now the conclusion is a direct consequence of Eq. (43) and of the divergence theorem.

Here again, one straighforwardly checks that the conservation of momentum is satisfied. We have in particular

$$(Lv_0, w) = \frac{1}{\sigma^2}\int_{\partial\Omega_1}\left(\frac{1}{2} - I_1\right)\left\langle (d_{\varphi^v_{10}}\varphi^v_{01})^* \nu_1,\ w \circ \varphi^v_{10}(x)\right\rangle d\sigma_1(x)$$

Letting $\mu_0 = \varphi^v_{01}(\sigma_1)$, and $\nu_0(x) = (d_x\varphi^v_{01})^* \nu_1 \circ \varphi^v_{10}(x)$ this can be rewritten

$$(Lv_0, w) = \frac{1}{\sigma^2}\int_{\partial\Omega_0}\left(\frac{1}{2} - I_1 \circ \varphi^v_{01}(x)\right)\langle v_0, w\rangle d\mu_0(x)$$

which is under the general form of a measure-based momentum.

5.4.3. Inexact Image Matching—In this section, we let I_0 and I_1 be two smooth enough (say C^1) functions defined on Ω (images). We consider the image matching problem which corresponds to minimizing, over G,

$$U(\varphi) = E(\varphi) + \frac{1}{\sigma^2}\int_\Omega |I_0 \circ \varphi^{-1}(x) - I_1(x)|^2 dx$$

This problem is equivalent to minimizing

$$\int_0^1 \|v_t\|_L^2 dt + \frac{1}{\sigma^2}\int_\Omega |I_0 \circ (\varphi^v_{01})^{-1}(x) - I_1(x)|^2 dx$$

This matching problem has been studied, in particular in [4], to show that the optimal solution should satisfy, at each time t,

$$Lv_t = -\frac{1}{\sigma^2}|d\varphi^v_{t,1}|(I^v_{0t} - I^v_{1t})\nabla I^v_{0t} \tag{45}$$

in which we have introduced the notation: $I^v_{0t} = I_0 \circ \varphi^v_{t0}$, $I^v_{1t} = I_1 \circ \Phi^v_{t1}$, and $|d\varphi|$ for the Jacobian of φ. This equation is in fact an equation of conservation of momentum, with

$$Lv_0 = -\frac{1}{\sigma^2}|d\varphi^v_{01}|(I_0 - I^v_{10})\nabla I_0$$

as can be deduced from Eq. (30), with $\alpha = -\frac{1}{\sigma^2}|d\varphi^v_{01}|(I_0 - I^v_{10})$. Moreover, we can check also the normality property (31) which holds here with with $r = 1$ and $f_0 = I_0$. This allows us to conclude that for the geodesic path in the image space generated by inexact matching, the lifting of the path in G defines a geodesic for which the momentum stays normal to the level sets of the current image $I_0 \circ \varphi_{t,0}$ at time t.

6. Geodesic Evolution in the Orbit

Thus far we have concentrated on the evolution of the flow of diffeomorphisms and its conservation of momentum. For all of our image understanding work we use the flow (φ_t, $t \in [0, 1]$) to act on the elements in the orbits $\mathcal{I}$ of a given template $I = I_{\text{temp}}$. Now we examine the geodesic flows in the orbit $\{I_t = I \circ \varphi_t, t \in [0, 1]\}$, $I \in \mathcal{I}$, and provide the associated evolution equations.

6.1. Geodesic Evolution Equation of Landmark Points

Here we examine the finite dimensional landmark orbit denoted $\mathcal{I}_n$, consisting of n-shapes $I_N = (x_1, \ldots, x_n)$, each landmark $(x_i)_{1\le i\le n}$ is in $\Omega \subset \mathbb{R}^d$; correspondingly $(a_i)_{1\le i\le n}$ are a finite family of vectors in $\mathbb{R}^d$. Denoting by $x_i(t) \doteq \varphi_t(x_i)$, the trajectory in Ω of the point x_i under the flow φ_t gives

$$Lv_t = \sum_{i=1}^{n} \delta^*_{x_i(t)} a_i(t), \tag{46}$$

where $a_i(t) = (d_{x_t}(t)\,\varphi_{t,0})^* a_i$. From the identity

$$\frac{d}{dt}((d_{x_i(t)}\varphi_{t,0})^*) = -\,d_{x_i(t)}v_t^*(d_{x_i(t)}\varphi_{t,0})^*, \tag{47}$$

we deduce that $\frac{da_i}{dt}(t) + (d_{x_i(t)}v_t)^* a_i(t) = 0$. To prove (47), one needs to remark that

$$d_{x_i(t)}\varphi_{t,0} = d_{\varphi_{0,t}(x_i)}\varphi_{t,0} = (d_{x_i}\varphi_{0,t})^{-1}$$

Now,

$$\begin{aligned}\frac{d}{dt}(d_{x_i}\varphi_{0,t})^{-1} &= -\,(d_{x_i}\varphi_{0,t})^{-1}\frac{d}{dt}(d_{x_i}\varphi_{0,t})(d_{x_i}\varphi_{0,t})^{-1}\\ &= -\,(d_{x_i}\varphi_{0,t})^{-1}(d_{\varphi_{0,t}(x_i)}v_t d_{x_i}, \varphi_{0,t}) \times (d_{x_i}\varphi_{0,t})^{-1}\\ &= d_{x_i(t)}\varphi_{t,0} d_{x_i(t)}v_t\end{aligned}$$

Hence we get the following geodesic evolution in the orbit of landmarks.

Proposition 3 (Landmark Transport)—The landmarks are transported along the geodesic according to the following equations with velocity vector field satisfying

$$v_t = L^{-1}\left(\sum_{i=1}^{n} \delta^*_{x_i(t)} a_i(t)\right) = \sum_{i=1}^{n} K(x_i(t), \cdot) a_i(t)$$

where K(x, y) is the Green kernel associated with L:[3]

$$\begin{cases} \frac{da_i}{dt}(t)+(d_{x_i(t)}v_t)^* a_i(t)=0, \\ \frac{dx_i}{dt}(t) - v_t(x_i(t))=0. \end{cases} \tag{49}$$

Note that the expression of v_t from Eq. (48) can be introduced into the system (49), yielding an evolution equation which only depends on the landmarks in the orbit.

We notice the reduction of the vector field to the range space of the Green's kernels travelling over the landmark trajectories is as in [17].

There is a straightforward extension of this result to *geodesic curve evolution*, in which $x(0)$ is a parametrized curve $\sigma \mapsto x(\sigma)$ for $\sigma \in [0, L]$ and

$$Lv_0=\int_0^L \delta^*_{x(0,\sigma)} v_0(\sigma)d\sigma$$

where $v_0(\sigma)$ is normal to $x(0)$. In this case, we have

$$Lv_t=\int_0^L \delta^*_{x(t,\sigma)} v_t(\sigma)d\sigma$$

with

- $\frac{\partial v_t}{\partial t}(t,\sigma)+(d_{x(t,\sigma)}v_t)^* v(t,\sigma)=0$,
- $\frac{\partial x}{\partial t}(t,\sigma) - v_t(x(t,\sigma)=0$.

6.2. Geodesic Image Evolution

Assume here that $d\mu = \alpha(x)dx$ has a density with respect to Lebesgue's measure on Ω. In this case, $d\mu_t = |d\varphi_{t0}|\alpha \circ \varphi_{t0}dx$ and

$$Lv_t=|d\varphi_{t0}|\alpha \circ \varphi_{t0}\nabla I_t \tag{50}$$

From the conservation of momentum in Lagrangian coordinates for image based motion, we get for $Lv_0 = \alpha_0 \nabla I_0$ that $Lv_t = \alpha_t |d\varphi_{t,0}|\nabla I_t$ where $\alpha_t = \alpha_0 \circ \varphi_{t,0}$, $I_t = I_0 \circ \varphi_{t,0}$. Let $z_t = \alpha_t |d\varphi_{t,0}|$ so that $Lv_t = z_t \nabla I_t$.

Since $\frac{d}{dt}(z_t \circ \varphi_{0,t})=\frac{d}{dt}(|d_{\varphi 0,t}\varphi_{t,0}|\alpha_0)= - \operatorname{div}(v_t) \circ \varphi_{0,t}|d_{\varphi 0,t}\varphi_{t,0}|\alpha_0$ we get $\frac{dz_t}{dt}+dz_t(v_t)+\operatorname{div}(v_t)z_t$. Moreover, we get easily $\frac{\partial I_t}{\partial t}+\langle \nabla I_t, v_t\rangle=0$. Hence we get the following geodesic evolution equation in image space.

---

[3]The explicit form for L^{-1} depending on the kernel K is defined as follows. For any $x, y \in \Omega$, the bilinear form $K_{x,y}$ on $\mathbb{R}^d \times \mathbb{R}^d$ defined by

$$K_{xy}(a,b) \doteq \langle \delta^*_x a, \delta^*_y b\rangle_{g^*}=(\delta^*_y b, L^{-1}(\delta^*_x a))=\langle L^{-1}(\delta^*_x a)(y), b\rangle_{\mathbb{R}^d} \tag{49}$$

Proposition 4 (Image Transport)—The image is transported along the geodesic according to the following equations: with vector field $v_t = L^{-1}(z_t \nabla I_t)$:

- $\frac{dz_t}{dt} + dz_t(v_t) + \mathrm{div}(v_t) z_t = 0,$
- $\frac{\partial I_t}{\partial t} + \langle \nabla I_t, v_t \rangle = 0.$

Notice that these equations appear as a limit case of the evolution equations which have been studied in [34] for image comparison.

As illustrated above, the pair (I_0, μ) provides a device for modeling deformations. In the cases we have studied, I_0 was representing some geometrical structure (a curve, an image), which evolved with time accordi to the generated deformation, and μ, essentially quantifies the speed and direction of the deformation.

We get from this a natural way to represent the deformation of a template. Using Grenander's original terminology, I_0 would precisely be the template and μ is the generator of the deformation. Thus, fixing I_0, and letting μ vary, we get a model which represents perturbations of the template.

An example of deformations of an image is provided in Fig. 2. The images have been obtained by solving Eq. (50) from an initial image g of a slice of macaque brain, and taking

$$\alpha(x) = \frac{X(x)}{1 + |\nabla_x I_0|}$$

where X is a Gaussian process.

7. Computational Results

The following results illustrate the computation of the momentum $Lv_0 = \alpha_0 \nabla I_0$ (as described in Section 6.2) from geodesic paths between two images. These geodesics are computed using F. Beg's implementation of image matching, as described in [4]. In these experiments, the operator L is $(\nabla + c \text{ Identity})$,[2] implemented via fast Fourier transform. The shooting algorithm solves the equation provided in Proposition 4 with initial condition $(I_0, z_0 = \alpha_0)$.

Figure 3 shows the three objects studied, a smooth Gaussian bump for shift, circles for scale, and two mitochondria examin g both forward and inverse shooting.

Shown in Fig. 4–6 are examples illustrating the image based momentum and the diffeomorphisms generated via geodesic shooting. Figure 4 shows the results of the translation experiment. Panels 1 and 2 show I_0 and I_1; panel 3 shows the diffeomorphism generated via geodesic shooting applied to I_0, and illustrates how solving the conservation of momentum equation allows to recover I_1 from I_0 and Lv_0.

Shown in panel 4 is the density α showing the concentration near the boundary of I_0. Superposed in panel 5 are the predicted directions of the momentum, given by $\alpha_0 \nabla I_0$, and the value Lv_0 obtained from Beg's algorithm. In almost all case they appear as one line indicating a good accuracy of the algorithm. Panel 6 indicates that the vector field V_0 demonstrating that while α and the momentum Lv_0 are highly localized, the velocity of motion extends over the entire object.

Shown in Fig. 5 are similar results for the scale experiment.

Shown in Fig. 6 are two sets of results for the geodesic shooting of the mitochondria. The organization of the results are the same as for the translation and scale experiments. Shown in Fig. 6 are two sets of results for the geodesic shooting of the mitochondria. The organization of the results are the same as for the translation and scale experiments.

Acknowledgments

Michael I. Miller was supported by grants from the National Institute of Wealth numbers P41-RR15241-01A1, U24-RR0211382-01, P20-MH071616-01.

References

1. Arnold, VI. Mathematical Methods of Classical Mechanics. 1. Springer; 1978. 1989
2. Arnold V, Khesin B. Topological methods in hydrodynamics. Ann Rev Fluid Mech 1992;24:145–166.
3. Arnold VI. Sur la géometrie differentielle des groupes de Lie de dimension infinie et ses applications à l'hydrodynamique des fluides parfaits. Ann Inst Fourier (Grenoble) 1966;1:319–361.
4. Beg MF, Miller MI, Trouvé A, Younes L. Computing large deformation metric mappings via geodesics flows of diffeomorphisms. Int J Comp Vis February;2005 61(2):139–157.
5. Camion, V.; Younes, L. Geodesic interpolating splines. In: Figueiredo, MAT.; Zerubia, J.; Jain, AK., editors. EMM-CVPR 2001, Vol. 2134 of Lecture Notes in Computer Sciences. Springer-Verlag; 2001. p. 513-527.
6. Chen, T.; Metaxas, D. Medical Image Computing and Computer-Assisted Intervention—Miccai 2000, Vol. 1935 of Lecture Notes in Computer Science. Springer-Verlag; 2000. Image segmentation based on the integration of Markov random fields and deformable models; p. 256-265.
7. Christensen GE, Rabbitt RD, Miller MI. Deformable templates using large deformation kinematics. IEEE Trans Image Processing 1996;5(10):1435–1447.
8. Cohen I, Cohen L, Ayache N. Using deformable surfaces to segment 3-d images and infer differential structures. Computer Vision Graphics Image Processing 1992;56(2):242–263.
9. Cootes T, Taylor C, Cooper D, Graham J. Active shape models—Their training and application. Comp Vision and Image Understanding 1995;61(1):38–59.
10. Delfour, MC.; Zolésio, J-P. Shapes and Geometries. Analysis, Differential Calculus and Optimization. SIAM; 2001.
11. Dupuis P, Grenander U, Miller M. Variational problems on flows of diffeomorphisms for image matching. Quart App Math 1998;56:587–600.
12. Garrido A, De la Blancà NP. Physically-based active shape models: Initialization and optimization. Pattern Recognition 1998;31(8):1003–1017.
13. Grenander, U. General Pattern Theory. Oxford Univeristy Press; 1994.
14. Grenander, U.; Chow, Y.; Keenan, D. HANDS: A Pattern Theoretic Study of Biological Shapes. Springer-Verlag; New York: 1990.
15. Grenander U, Miller MI. Representations of knowledge in complex systems. J Roy Stat Soc B 1994;56(3):549–603.
16. Grenander U, Miller MI. Computational anatomy: An emerging discipline. Quart App Math 1998;56:617–694.
17. Joshi S, Miller MI. Landmark matching via large deformation diffeomorphisms. IEEE Trans Image Processing 2000;9(8):1357–1370.
18. Kass M, Witkin A, Terzopolous D. Snakes: Active contour models. International Journal of Computer Vision 1988;1(4):321–331.
19. Marsden, JE.; Ratiu, TS. Introduction to Mechanics and Symmetry. Springer; 1994.

20. Mignotte M, Meunier J. A multiscale optimization approach for the dynamic contour-based boundary detection issue. Computerized Medical Imaging and Graphics 2001;25(3):265–275. [PubMed: 11179703]
21. Miller, M.; Joshi, S.; Maffitt, DR.; McNally, JG.; Grenander, U. Mitochondria, membranes and amoebae: 1, 2 and 3 dimensional shape models. In: Mardia, K., editor. Statistics and Imaging. Vol. II. Carfax Publishing; Abingdon, Oxon: 1994.
22. Miller M, Trouvé A, Younes L. On the metrics and Euler-Lagrange equations of computational anatomy. Annual Review of Biomedical Engineering 2002;4:375–405.
23. Miller M, Younes L. Group actions, homeomorphisms, and matching: A general framework. International Journal of Computer Vision 2001;41(1/2):61–84.
24. Montagnat, J.; Delingette, H. Cvrmed-Mrcas'97, Vol. 1205 of Lecture Notes in Computer Science. Springer-Verlag; 1997. Volumetric medical images segmentation using shape constrained deformable models; p. 13-22.
25. Montagnat J, Delingette H, Ayache N. A review of deformable surfaces: Topology, geometry and deformation. Image and Vision Computing 2001;19(14):1023–1040.
26. Mumford, D. Questions Mathématiques En Traitement Du Signal et de L'Image. Vol. Chap 3. Institut Henri Poincaré; 1998. Pattern theory and vision; p. 7-13.
27. Osher S, Sethian JA. Front propagating with curvature dependent speeds: Algorithms based on Hamilton-Jacobi formulation. Journal of Comp Physics 1988;79:12–49.
28. Pham D, Xu C, Prince J. Current methods in medical image segmentation. Ann Rev Biomed Engng 2000;2:315–337. [PubMed: 11701515]
29. Schultz N, Conradsen K. 2d vector-cycle defonnable templates. Signal Processing 1998;71(2):141–153.
30. Sclaroff S, Liu LF. Deformable shape detection and description via model-based region grouping. IEEE Transactions on Pattern Analysis and Machine Intelligence 2001;23(5):475–489.
31. Staib L, Duncan J. Boundary finding with parametrically deformable models. IEEE Trans Pattern Analysis and Machine Intelligence 1992;14:1061–1075.
32. Staib L, Duncan J. Model-based deformable surface finding for medical images. IEEE Trans Medical Imaging 1996;15(5):1–13.
33. Terzopoulos D, Metaxas D. Dynamic models with local and global deformations: Deformable superquadrics. IEEE Trans Patt Anal Mach Intell 1991;13:703–714.
34. Trouvé A, Younes L. Local geometry of deformable template. SIAM Journal of Mathmatical Analysis. to appear.
35. Trouvé A. Action de groupe de dimension infinie et reconnaissance de formes. CR Acad Sci Paris, Série I, No 321 1995:1031–1034.
36. Trouvé A. Diffeomorphisms groups and pattern matching in image analysis. Int J Computer Vision 1998;28:213–221.
37. Vaillant M, Davatzikos C. Finding parametric representations of the cortical sulci using an active contour model. Medical Image Analysis 1997;1(4):295–315. [PubMed: 9873912]
38. Westin, CF.; Lorigo, LM.; Faugeras, O.; Grimson, WEL.; Dawson, S.; Norbash, A.; Kikinis, R. Medical Image Computing and Computer-Assisted Intervention—MICCAI 2000, Vol. 1935 of Lecture Notes in Computer Science. Springer-Verlag; 2000. Segmentation by adaptive geodesic active contours; p. 266-275.
39. Xu, C.; Pham, DL.; Prince, JL. Finding the brain cortex using fuzzy segmentation, isosurfaces and deformable surface models. XVth Int. Conf. on info Proc. in Medical Imaging; June 1997;
40. Xu, C.; Pham, DL.; Prince, JL. Medical image segmentation using deformable models. In: Fitzpatrick, J.; Sonka, M., editors. SPIE Handbook on Medical Imaging - Volume III: Medical Image Analysis. SPIE; Bellingham, WA: 2000. p. 129-174.
41. Xu C, Prince JL. Gradient vector flow: A new external force for snakes. CVRP. Nov;1997
42. Xu, C.; Prince, JL. Gradient vector flow deformable models. In: Bankman, I., editor. Handbook of Medical Imaging. Academic Press; San Diego, CA: 2000.

43. Yezzi A, Tsai A, Willsky A. A fully global approach to image segmentation via coupled curve evolution equations. Journal of Visual Communication and Image Representation 2002;13(1–2): 195–216.

Appendix A: Proof of Theorem 3

Proof

Since $g_{I_t}^{\perp}$ is closed, we have to show that for almost all t, $v_t = p_{I_t}(v_t)$. Denote $h_t \doteq v_t - p_{I_t}(v_t)$. For $\varepsilon \in [0, 1]$, let $v_t^{\varepsilon} \doteq v_t + \varepsilon h_t$, and $\varphi_t^{\varepsilon} \doteq \varphi_t^{v^{\varepsilon}}$ (one can check, but we skip the argument, that $t \to h_t$ is measurable and belongs to $L^2([0, 1], \mathcal{g})$, so that this variation is valid).

The proof essentially consists in showing that, for all $0 \le t \le 1$

$$I_0 \circ \varphi_{t0} = I_0 \circ \varphi_{t0}^{\varepsilon}. \tag{51}$$

Indeed, assume that this result is proved. Considering $\varepsilon = 1$ and $t = 1$, we deduce that $I_1 = I_0 \circ \varphi_{1,0}^{1}$. However, since $\langle h_t, v_t \rangle_L = \langle v_t - p_{I_t}(v_t), v_t \rangle_L = 0$, we get $|v_t + h_t|_L^2 = |v_t|_L^2 - |h_t|_L^2$. Since $t \to v_t$ corresponds to paths with lowest kinetic energy from I_0

to I_1, we deduce that $\int_0^1 |h_t|_L^2 dt = 0$ and the proof is ended.

We now return to Eq. (51). Using the formula

$$\frac{d\varphi_{t0}(x)}{dt} = -d_x \varphi_{t0} v_t(x)$$

and letting $q_t^{\varepsilon}(x) = \varphi_{t0} \circ \varphi_{0t}^{\varepsilon}(x)$, we obtain

$$\begin{aligned} \frac{\partial q_t^{\varepsilon}(x)}{\partial t} &= -d_{\varphi_{0t}^{\varepsilon}(x)} \varphi_{t0} v_t \circ \varphi_{0t}^{\varepsilon}(x) + d_{\varphi_{0t}^{\varepsilon}(x)} \varphi_{t0}(v_t \circ \varphi_{0t}^{\varepsilon}(x) + \varepsilon h_t \circ \varphi_{0t}^{\varepsilon}(x)) \\ &= \varepsilon d_{\varphi_{0t}^{\varepsilon}(x)} \varphi_{t0} h t \circ \varphi_{0t}^{\varepsilon}(x) \end{aligned}$$

We first prove Eq. (51) under the assumption that I_0 is C^1. From the computation above, we have

$$\begin{aligned} \frac{\partial}{\partial t}(I_0 \circ q_t^{\varepsilon})(x) &= \varepsilon \left\langle \nabla_{\varphi_{t0}(\varphi_{0t}^{\varepsilon}(x))} I_0, d_{\varphi_{0t}^{\varepsilon}(x)} \varphi_{t0} h_t \circ \varphi_{0t}^{\varepsilon}(x) \right\rangle_{\mathbb{R}^d} \\ &= \varepsilon \left\langle \nabla_{\varphi_{0t}^{\varepsilon}(x)} I_t, h_t(\varphi_{t0}^{\varepsilon}(x)) \right\rangle_{\mathbb{R}^d} = 0 \end{aligned}$$

since by definition of the projection $p_{I_t}(v_t)$, we have for any $x \in \Omega$

$$\langle h_t(x), \nabla I_t(x) \rangle_{\mathbb{R}^d} = \langle v_t(x), \nabla I_t(x) \rangle_{\mathbb{R}^d} - \langle p_{I_t}(v_t), \nabla I_t(x) \rangle_{\mathbb{R}^d} = 0.$$

This implies $I_0 \circ \varphi_{t,0} \circ \varphi^{\varepsilon}_{0,t} = I_0$ which yields Eq. (51) in this case. When I_0 is not smooth, the proof goes by showing that

$$\frac{\partial}{\partial t} \int_\Omega I_0 \circ q^{\varepsilon}_t(x) f(x) dx = \int_\Omega I_t(x) \mathrm{div}(h_t g^{\varepsilon}_t)(x) dx$$

for smooth f on Ω and $g^{\varepsilon}_t \circ \varphi^{\varepsilon}_t |d\varphi^{\varepsilon}_t| = f$ which can be done either by a direct (heavy) computation, or by using a density argument, based on the fact that, by the divergence theorem, this is true for smooth I_0 (we skip the details).

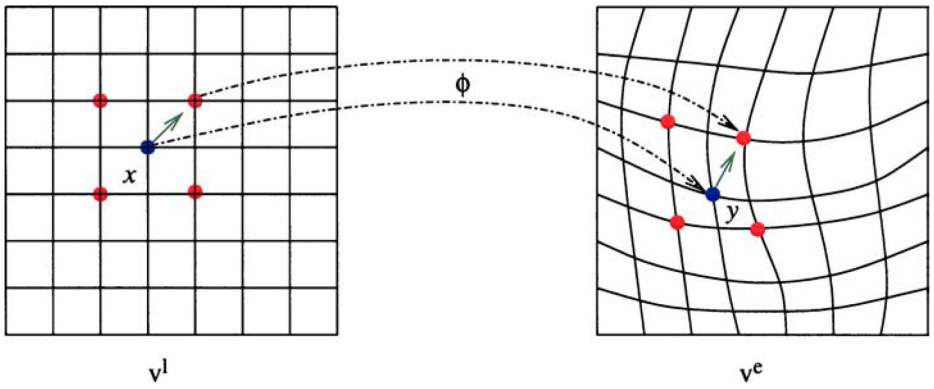

Figure 1.
Here is represented the deformation obtained by pulling back the Eulerian frame associated with v^e and represents pictorially the adjoint action.

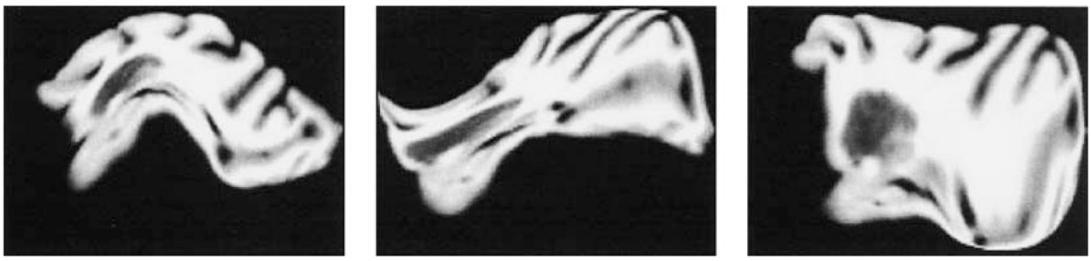

Figure 2.
Three random deformations of an image.

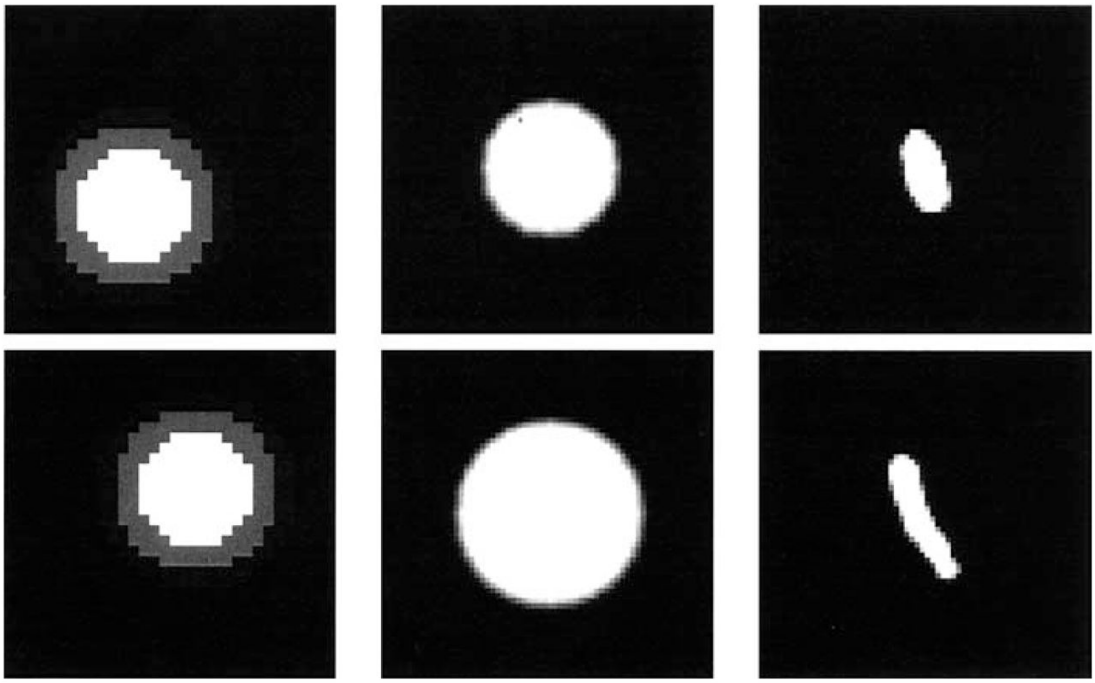

Figure 3.
Figure shows objects under translation (column 1), scale (column 2), and mitochondria 1 and 2.

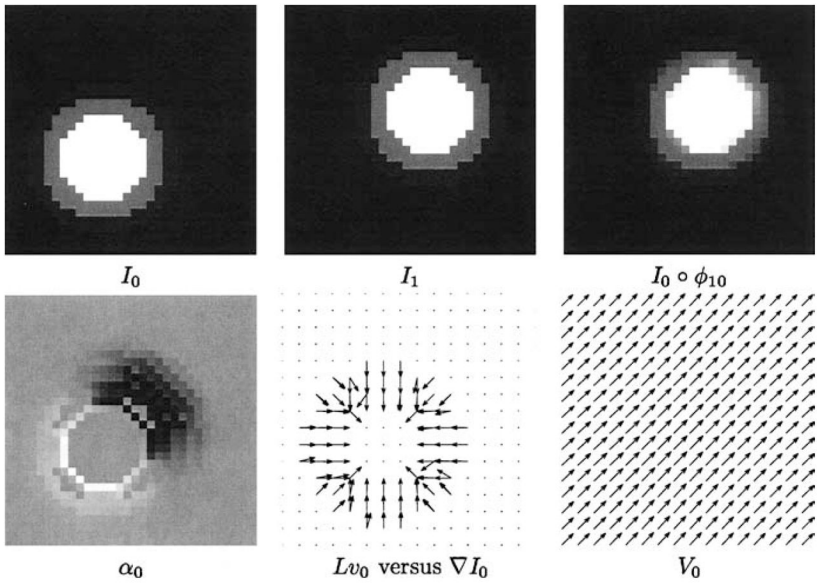

Figure 4.
Rows 1, 2: Results from translation experiment. Panels 1, 2, and 3 show I_0, I_1, $I_0 \circ \varphi_{10}$. Panels 4, 5 and 6 show α_0, Lv_0 versus $\alpha_0 \nabla I_0$, and V_0 and $L^{-1}\alpha \nabla I_0$.

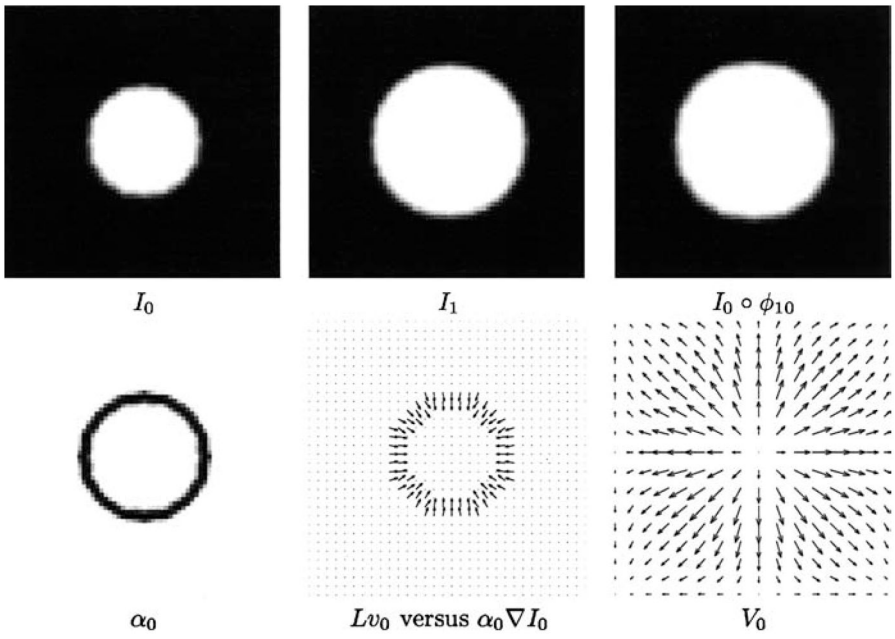

Figure 5.
Rows 1, 2: Results from scale experiment. Panels 1, 2, and 3 show I_0, I_1, $I_0 \circ$; φ_{10}. Panels 4, 5 and 6 show α_0, Lv_0 versus $\alpha_0 \nabla I_0$, and V_0 and $L^{-1}\alpha \nabla I_0$.

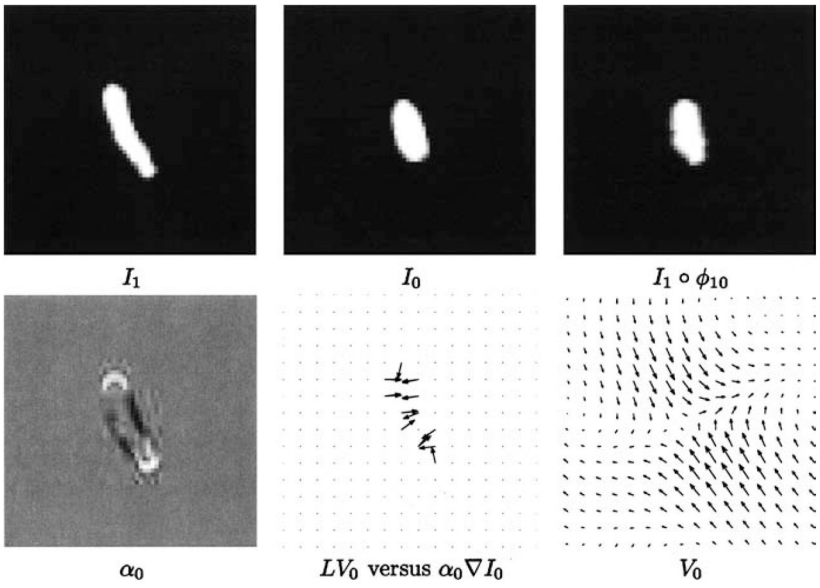

Figure 6.
Results from mitochondria 2. Panels 1, 2, and 3 show I_1, I_0, $I_1 \circ \varphi_{10}$. Panels 4, 5 and 6 show α_0, LV_0 versus $\alpha_0 \nabla I_0$, and V_0.

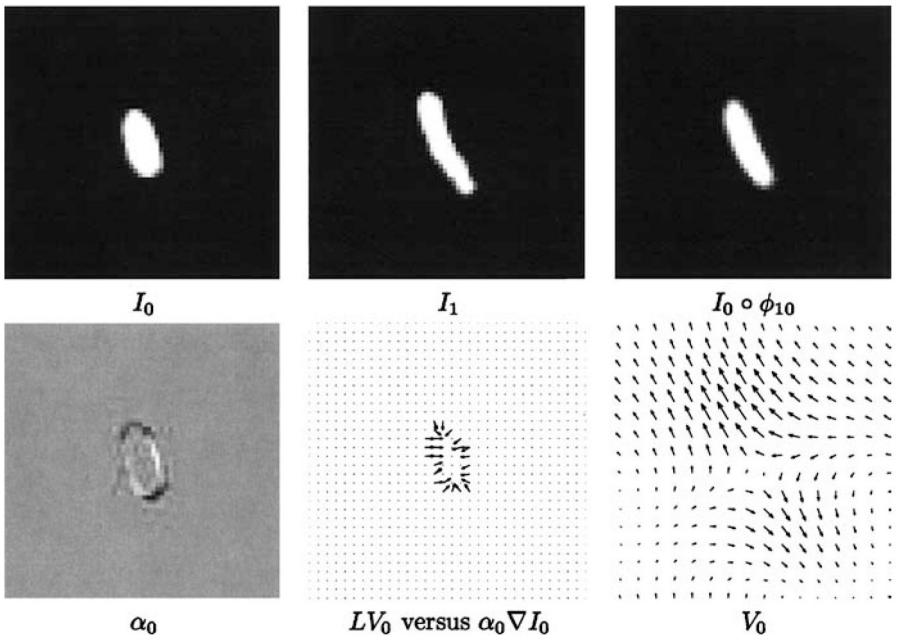

Figure 7.
Results from mitochondria 1. Panels 1, 2, and 3 show I_0, I_1, $I_0 \circ \varphi_{10}$. Panels 4, 5 and 6 show α_0, LV_0 versus $\alpha_0 \nabla I_0$, and V_0.